

Water Vapour and Its Role in the Earth's Greenhouse*

Graeme L. Stephens^A and *Stephen A. Tjemkes*^B

^A Department of Atmospheric Science, Colorado State University,
Fort Collins, CO 80523, U.S.A.

^B Institute for Meteorology and Oceanography, State University of the Netherlands,
Princetonplein 5, 3584 CC Utrecht, The Netherlands.

Abstract

This paper examines the role of water vapour as a greenhouse gas and discusses its role in the evolution of the atmospheres of Venus, Earth and Mars. The paper focuses on how the greenhouse effect operates on Earth and describes the feedback between temperature and water vapour that is thought to play a key role in global warming induced by increasing concentrations of carbon dioxide. A method for analysing the contribution of water vapour to the greenhouse effect using satellite observations is discussed. It is shown how this contribution varies in a directly proportional way with the amount of water vapour vertically integrated through the column of the atmosphere. Based on the results obtained from the analyses of satellite data, it is established that the sensitivity of the greenhouse effect to changing sea surface temperature is not uniform over the globe and is significantly greater over warmer oceans. The relevance of the results to the water vapour feedback is discussed.

1. The Greenhouse Effect

A balance between the amount of sunlight absorbed by the planet and the radiation emitted to space is the primary climate control of Earth. Most of the solar energy that reaches the Earth is absorbed at the surface of the Earth. The surface, warmed by this absorbed sunlight, emits radiation towards space at longer (infrared) wavelengths (sometimes referred to as longwave or terrestrial radiation). Certain gases, such as water vapour and carbon dioxide, together with clouds strongly absorb this emitted radiation. These atmospheric constituents, in turn, re-emit longwave radiation at temperatures that are lower than the surface temperature. The absorption and re-emission of longwave radiation in the atmosphere provides an effective mechanism for blocking the surface emission from escaping directly to space and helps maintain higher temperatures than otherwise occur in the absence of an atmosphere. This blocking or trapping mechanism is the so-called greenhouse effect. In the analogy between the planet and a greenhouse illustrated in Fig. 1, the glass of the greenhouse is supposed to serve the same function as the planet's atmosphere. Solar radiation is transmitted through the transparent glass into the greenhouse and the longwave radiation emitted by all objects in the greenhouse is blocked by the glass which is opaque to this longwave radiation. This analogy, however, is itself a topic of debate (Bohren 1987).

* Paper presented at the Tenth AIP Congress, University of Melbourne, February 1992.

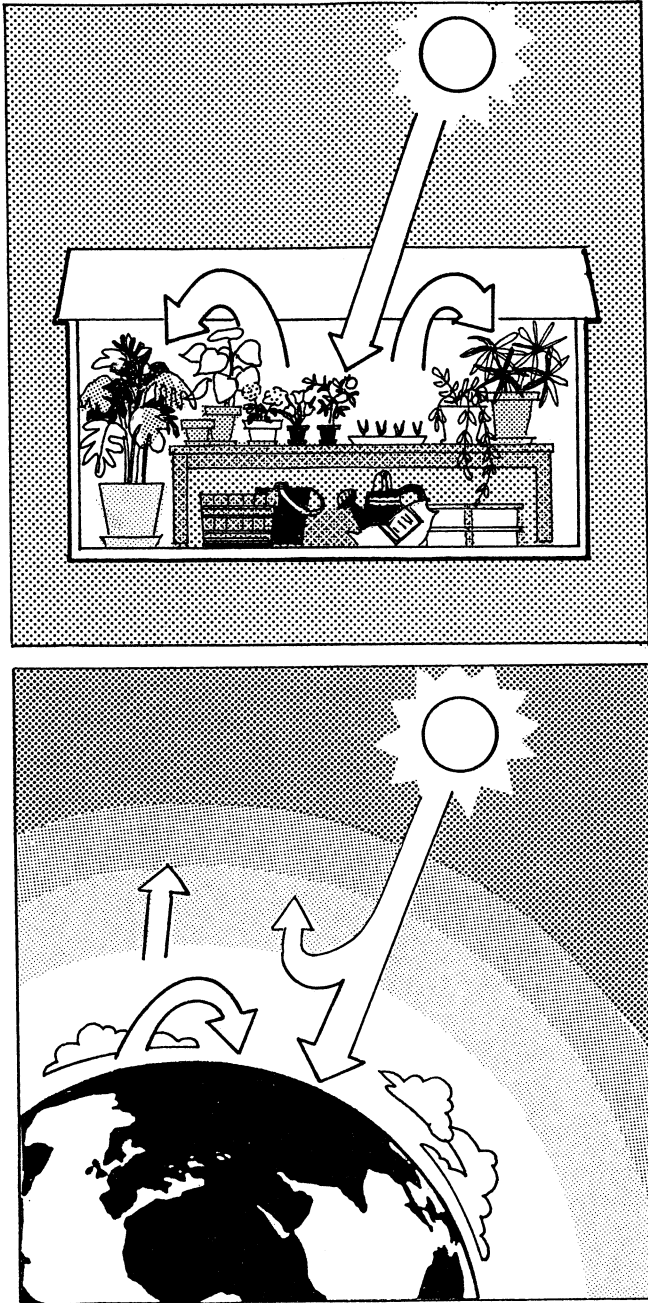


Fig. 1. The greenhouse effect of Earth: approximately 70% of the incoming solar radiation is absorbed at the Earth's surface. The remaining 30% is reflected back to space through a combination of surface reflection and reflection by the Earth's atmosphere, largely through the presence of clouds. The radiation emitted by the Earth's surface occurs at longer (infrared) wavelengths and is largely trapped in the atmosphere through absorption by trace gases such as water vapour and carbon dioxide and by cloud particles. As a result, less longwave radiation is emitted to space than is emitted at the surface. These processes occur in a manner supposedly analogous to a greenhouse where the glass of the greenhouse serves the same function as the Earth's atmosphere.

Knowledge of the greenhouse effect is fundamental to our understanding of how atmospheres evolved in the past and, in particular, how the Earth's atmosphere is likely to evolve in the future. Fourier (1787) first pointed out that human activity can modify climate through this effect. The formal foundation of the greenhouse theory of climate change was established by Arrhenius (1896), who studied what is now the contemporary topic of the effects of increasing carbon dioxide on the greenhouse effect, and Callender (1938) provided one of the earliest attempts to quantify the effect of increasing carbon dioxide on the greenhouse effect.

Perhaps the simplest quantitative way of estimating the strength of the greenhouse effect as it occurs on Venus, Earth and Mars is in terms of a quantity referred to as the effective temperature of the planet. This temperature is defined in the following manner. The net sunlight absorbed by the planet is expressed as

$$\text{energy absorbed} = \pi R_e^2 Q_o (1 - \alpha), \quad (1)$$

where R_e is the radius of the planet and πR_e^2 is the cross sectional area projected by the planet that intercepts the flux of solar radiation Q_o (flux is defined here as the flow of energy per unit time and unit cross-sectional area). The quantity Q_o , referred to as the solar constant, is itself a subject of intensive study. Satellite observations collected over the past decade, for example, reveal variability of Q_o on a number of time scales (Foukal 1990) which are obviously associated with solar activity. Not all the solar energy that reaches the Earth is actually absorbed by the planet. A fraction α , called the planetary albedo, is reflected to space. In the early part of this century, the albedo of Earth was estimated to be about 50% (Dines 1917). This value was refined in the middle of this century and estimated to be about 40%. Since the late 1960s and early 1970s, satellite observations have provided more reliable estimates of the albedo and its present value is determined to be about 30% (Vonder Haar and Suomi 1971; Stephens *et al.* 1981).

The total amount of longwave radiation emitted to space is

$$\text{energy radiated} = 4\pi R_e^2 \sigma T_e^4, \quad (2)$$

where σ is the Stefan-Boltzmann constant and T_e is the temperature at which the planet effectively radiates as a black body. For a planet in equilibrium, the incoming solar energy absorbed by the planet is exactly balanced by the longwave energy emitted by the planet. Equations (1) and (2) therefore provide us with a way of estimating T_e , namely

$$T_e = \left[\frac{Q_o(1 - \alpha)}{4\sigma} \right]^{1/4}. \quad (3)$$

Table 1 presents values of the solar constant Q_o , the albedo α and T_e for Venus, Earth and Mars as well as the mean distances of each of these planets from the sun. According to (3), the effective temperature of the planet is independent of its size and depends on both the albedo and the sun-planet distance through

its dependence on Q_o . Because of its high albedo, the effective temperature of Venus is similar to that of Earth even though Earth is farther from the sun.

Table 1. Physical properties of three inner planets of the solar system

Planet	Distance from sun (10^6 km)	Solar constant (W m^2)	Albedo	T_e (K)	T_s (K)	τ_F^*
Venus	108	2620	0.71	244	750	59
Earth	150	1367	0.31	253	288	0.9
Mars	228	593	0.17	216	220	~ 0

For a planet with an atmosphere that is transparent to longwave radiation, the surface temperature is equal to T_e . Therefore, the difference between T_e and the surface temperature T_s occurs as a direct result of the greenhouse effect and this difference serves as an indication of the strength of this effect. In reference to Table 1, the values of the mean surface temperatures of the planet are shown together with values of T_e deduced from measured albedos and known values of Q_o . The comparison of these temperatures suggests the presence of an intense greenhouse effect on Venus compared with that on Earth and an almost negligible effect on Mars. We now outline a more specific definition of the greenhouse effect involving both T_s and T_e .

2. A Simple Model of the Greenhouse Effect

(2a) Grey Body Optical Depth of the Atmosphere

While it is useful to think of the greenhouse effect in terms of the difference between the surface and planetary temperatures, we will show here how it is perhaps more appropriate to define the greenhouse effect in terms of a parameter called the optical depth of the atmosphere. This parameter enters directly into our mathematical descriptions of how both solar and longwave radiation are transferred from one layer to another layer in the atmosphere. In the case of longwave radiation transfer, the optical depth associated with these wavelengths provides us with a direct measure of how the infrared radiation is trapped by the atmosphere. This arises directly from the theory of radiative transfer which provides a relationship between the fraction of radiation that penetrates through a layer of the atmosphere and the optical thickness of that layer.

For convenience of discussion, we define the optical depth as

$$\tau_\lambda^* = \int k_\lambda \rho dz, \quad (4)$$

where k_λ is an attenuation coefficient at a specific wavelength λ , ρ is the density of the species that attenuates the radiation and the integration is performed throughout the entire depth of atmosphere. The optical depth defined in this way is a complicated function of wavelength, owing to the very uneven attenuation of radiation across the portion of the electromagnetic spectrum in question. In the Earth's atmosphere, attenuation of both solar and longwave radiation largely results from both absorption and scattering by atmospheric gases, cloud water droplets and ice crystals.

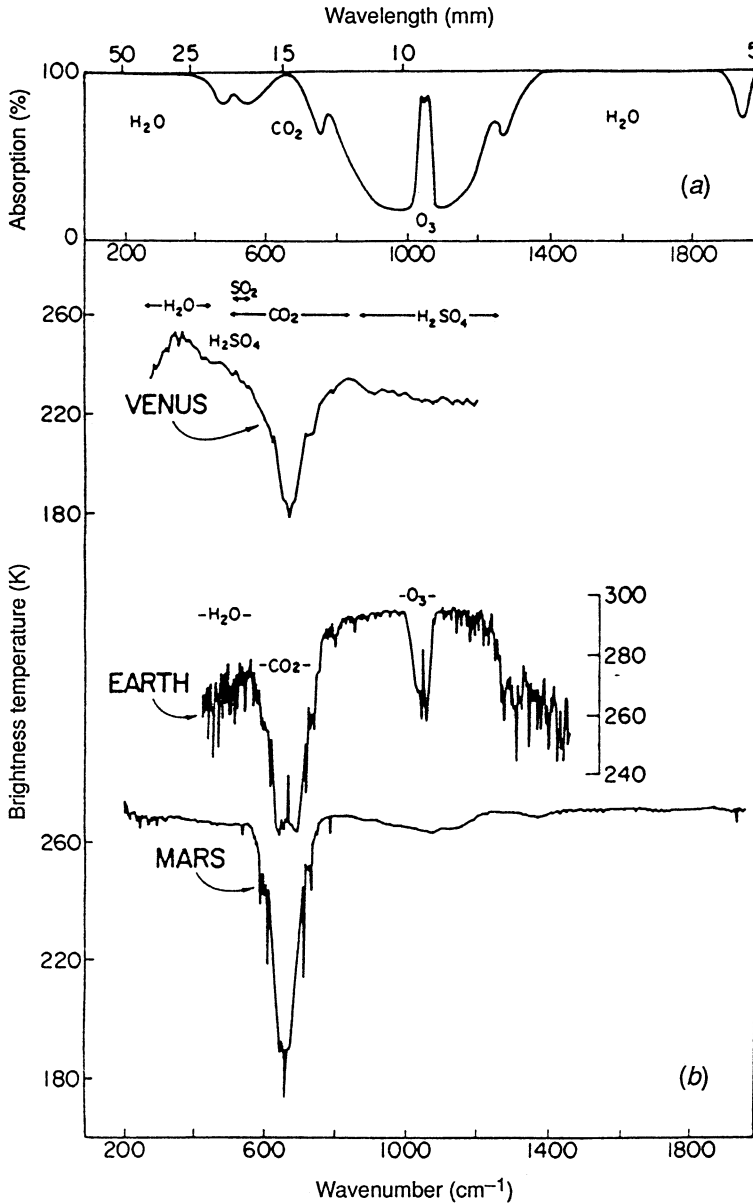


Fig. 2. (a) A low spectral resolution illustration of the absorption of longwave radiation by the main greenhouse gases in the Earth's atmosphere. (b) Spectra of emitted infrared radiation from Venus, Earth and Mars. The emitted radiation is expressed as brightness temperature and is in some sense related to the level in the atmosphere from which the radiation originates. The main greenhouse gases of the Earth's spectrum are highlighted; note the relatively transparent (i.e. warmer) region between about 880–1200 cm⁻¹ which is referred to as the atmospheric window. Here a satellite instrument sees almost directly down to the surface under clear skies. Sources: Hanel (1983) and Moroz *et al.* (1986).

Given the focus of this paper on the role of water vapour on the greenhouse effect for Earth, we choose to gloss over the importance of clouds, although we note that the attenuation by clouds is currently one of the most uncertain aspects of the Earth's greenhouse effect (Ramanathan 1988; Cess *et al.* 1990). We consider here the greenhouse effect that arises from the absorption and re-emission of the longwave radiation in the cloud-free atmosphere due to the presence of infrared-active gases (also referred to as greenhouse gases), principally water vapour with minor contributions by carbon dioxide, ozone and other trace gases.

A low spectral resolution depiction of the absorption of longwave radiation by the main infrared-active gases of the Earth's atmosphere is shown in Fig. 2*a*. Details of the absorption by these gases can also be inferred from the spectra of radiation emitted to space. Examples of spectra measured by radiometers flown on different spacecraft are shown in Fig. 2*b* for a clear-sky portion of Earth, for the cloudy skies over the mid-latitudes of Venus and for a dust-free region of the Martian atmosphere. Distinct absorption characteristics of the gases of the atmosphere can be identified in each spectrum. The Earth's clear-sky spectrum shows the broad spectral influence of water vapour emission as well as contributions by carbon dioxide primarily in a band of absorption lines centred about the wavelength of 15 μm . The spectrum for Mars essentially follows a black-body curve that is associated with the surface temperature of the planet, except at 15 μm , indicating that the Martian atmosphere is primarily composed of carbon dioxide. The 15 μm CO_2 band also appears as a dominant spectral signature in the emission spectra of Venus. Also evident in the Venusian spectrum are groups of water vapour and aerosol-phase H_2SO_4 features (Moroz *et al.* 1986).

The extreme spectral variability of absorption and emission by the atmospheres of the three inner planets shown in Fig. 2*b* means that the optical depth of the atmosphere as defined by (1) also varies from wavelength to wavelength and that a single spectrally averaged value of the optical depth can be a very ambiguous quantity. Nevertheless, we are able to derive a spectrally averaged optical depth that is of relevance to our study of the greenhouse effect. We introduce this quantity by assuming that a balance exists between the radiation emitted from the atmosphere integrated over all wavelengths and the spectrally integrated solar radiation absorbed by the planet (this is the same assumption invoked to derive T_e above). Under this assumption, we introduce an absorption coefficient that is weighted by the spectral flux of longwave radiation and averaged across the emission spectrum. Such an averaged quantity is referred to as the grey body absorption coefficient and there are several different ways to carry out this average (Mihalas 1978). In the context of radiative equilibrium we require that the grey body absorption coefficient be defined such that the grey body flux calculated from radiative equilibrium theory using this coefficient matches the spectrally integrated longwave flux emitted to space (Mihalas 1978). From this requirement we define an averaged absorption coefficient weighted to

$$k_F = H^{-1} \int k_\lambda H_\lambda d\lambda, \quad (5)$$

which is referred to as the flux-weighted mean absorption coefficient. In this definition, H_λ refers to the spectral flux of emitted radiation and H is the

spectral integral of this flux. In the case of water vapour we approximate the flux-weighted mean optical depth as

$$\tau_F^* = \int k_F \rho dz \approx k_F w, \quad (6)$$

where w is the vertically integrated amount of water vapour (meteorologists refer to this as the precipitable water or columnar water vapour, often expressed in the equivalent units of g cm^{-2} or in precipitable centimetres of water).

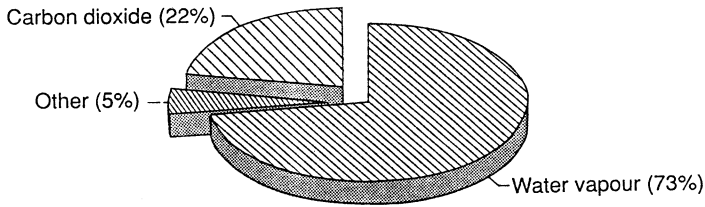


Fig. 3. A pie diagram illustrates the percentage of the grey body optical depth due to water vapour and other greenhouse gases in the Earth's atmosphere, based on typical mean global concentrations of these gases. The actual relative contributions of these gases vary significantly from place to place around the globe owing to an approximate five-fold change in the concentrations of water vapour from equator to pole.

The contributions to τ_F^* by water vapour, carbon dioxide and the other minor greenhouse gases present in the Earth's atmosphere are shown in Fig. 3. These contributions are based on calculations using concentrations of these gases that are considered typical of the atmosphere today. The spectral absorption data used to derive τ_F^* from (6) for water vapour, and its equivalent for the other gases, are taken from the 1980 version of the atmospheric absorption line parameters compiled by Rothman (1981). According to these calculations, the total grey body optical depth for all major greenhouse gases is calculated to be $\tau_F^* \approx 3.9$ with 73% of this being due to water vapour, 22% by CO_2 , and the remainder due to the collective contributions by ozone, nitrous oxide, methane and carbon monoxide. The value of $w = 2.8 \text{ g cm}^{-2}$ used to deduce the contribution by water vapour is close to its global mean value (Goody and Walker 1972). As we show below, the actual value of w varies substantially from place to place around the globe. In equatorial regions, values of w in excess of 5 g cm^{-2} are often observed, whereas values less than 1 g cm^{-2} are more typical of polar regions. Since CO_2 , N_2O and CH_4 are uniformly mixed in the atmosphere, the relative proportions of the contributions of these gases to τ_F^* also changes from place to place as the relative contribution of water vapour varies.

(2b) Grey Body Radiative Equilibrium

It is possible to derive a relationship between the temperature of the atmosphere and its grey body optical depth in a relatively simple way. We start by considering a very simple depiction of the atmosphere as shown in Fig. 4. The atmosphere is

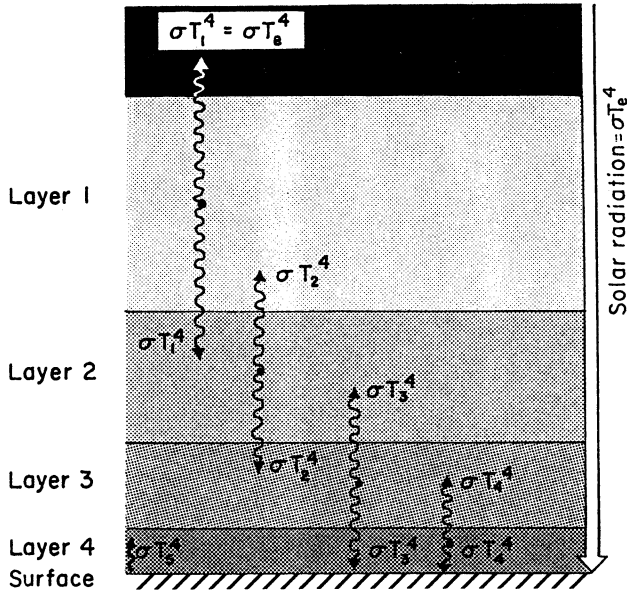


Fig. 4. Layers of the atmosphere that exchange IR radiation with adjacent layers. For this illustration, the atmosphere is taken to be transparent to solar radiation. The optical depth of each layer is the same but the geometric depth increases with altitude owing to the decreasing atmospheric density.

divided into several horizontal layers. The thickness of these layers varies in such a way that the radiation emitted by one layer is absorbed by the adjacent layer. Each layer is just thick enough to absorb all the radiation entering it. In this way each layer has the same optical depth τ_{layer} , which happens to correspond to the optical depth for which the transmission of the layer is effectively zero. The actual geometric thickness, however, increases with altitude since the density of the absorbing gas is less higher up in the atmosphere. The total number of such layers, N , then relates directly to the total optical depth of the atmosphere according to

$$\tau^* = N\tau_{layer} . \tag{7}$$

Suppose that each of these layers exists in a state of pure radiative equilibrium which means that the energy balance of each layer is determined only by the radiative balance of the layer. For the uppermost layer, this balance is expressed as

$$2\sigma T_e^4 = \sigma T_2^4 , \tag{8}$$

where the left-hand side of this expression is the emission from the layer (note that $T_e = T_1$) and the right-hand side is the longwave radiation absorbed by the

layer (we specifically neglect any absorption of solar radiation within the layer). In the same way we write the radiation balance of the second layer as

$$2\sigma T_2^4 = \sigma T_3^4 + \sigma T_1^4 \quad (9)$$

or as

$$\sigma T_3^4 = 3\sigma T_e^4 \quad (10)$$

with substitution from (8). It is straightforward to continue this type of analysis for N layers to obtain (Goody and Walker 1972).

$$\sigma T_s^4 = (1 + N)\sigma T_e^4 \quad (11)$$

or by using (7)

$$\sigma T_s^4 = (1 + b\tau^*)\sigma T_e^4, \quad (12)$$

where b is some constant that specifically relates to τ_{layer} . Derivations based on more sophisticated radiative transfer theory (Goody and Yung 1989; Mihalas 1978) yield the slightly modified form of (12)

$$\sigma T_s^4 = \sigma T_e^4 [a + b\tau^*], \quad (13)$$

where the specific assumptions of radiative transfer theory determine the constants a and b . From either the simple heuristic arguments given or the more elegant radiative transfer derivation of grey body equilibrium, we are able to arrive at a relationship between the surface temperature T_s and the planetary temperature T_e specifically in terms of the infrared grey body optical depth τ^* . This relationship therefore provides a way of conveniently defining the greenhouse effect in the following way:

$$\mathcal{G} = \frac{T_s^4}{T_e^4} = a + b\tau^*. \quad (14)$$

A specific form of this grey body radiative equilibrium model is found in the text of Goody and Yung (1989) in which case $a = 2$ and $b = 3/2$. Using this specific model, we estimate $\tau^* \approx 59$ for Venus and $\tau^* \approx 0.9$ for Earth (refer to Table 1).

The model represented by (14) has significant limitations when used to describe the state of the Earth's atmosphere. Firstly, the atmosphere is not a grey body, which is a point already appreciated by considering the absorption and emission spectra in Fig. 2. Secondly, the atmosphere of the Earth is not in a state of pure radiative equilibrium as implied by this model but rather is thought to be in a state of radiative and convective equilibrium. [A classic study of radiative-convective equilibrium is found in the paper of Manabe and Wetherald (1967).] This particular state of radiative and convective equilibrium provides a much reduced impact of the greenhouse effect on the surface temperature. Convection acts to mix heat up from the surface into the atmosphere, producing a cooler surface and warmer atmosphere. This reduction in the surface temperature by convection is the reason why we estimate a smaller value of τ^* in Table 1,

based on observed temperatures, than we derive from the pure radiative equilibrium arguments used to obtain the values relevant to Fig. 3. Another limitation of the simple model described above is that it assumes the atmosphere is completely transparent to solar radiation, whereas the clear atmosphere both scatters and absorbs approximately 10–20% of this energy. Despite these shortcomings, simple radiative equilibrium models of this type offer useful insight into how various atmospheric parameters, such as changes in the composition of the atmosphere, influence the climate in a very major way. Furthermore, we show below how expressions of the form (14) actually seem to represent certain aspects of the observed climate of Earth.

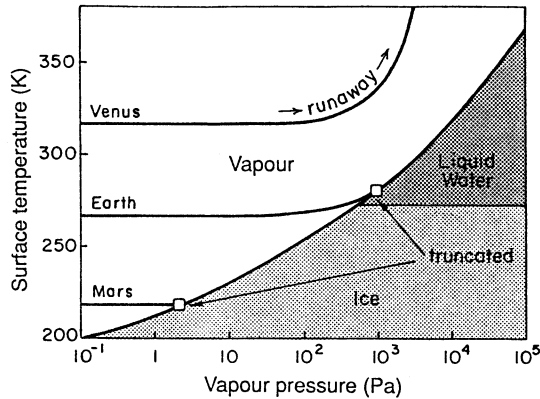


Fig. 5. World history lines of the surface temperature of the three inner planets as a function of increasing water vapour content. The history lines are shown on the phase diagram of water and illustrate runaway and truncated greenhouse effects. The curves show how the surface temperatures increase, due to the greenhouse effect, as water vapour accumulates in the atmosphere of the inner planets. On Earth and Mars the increase halted when the atmosphere reached a point of saturation leading to condensation and sublimation. Venus, being closer to the Sun, was originally warmer and saturation was never reached. It is conjectured that the temperature runs away in a manner that exemplifies a powerful water vapour feedback mechanism (from Rasool and DeBergh 1990).

3. Evolutionary Theories of the Atmosphere: A Case for Water Vapour Feedback

Theories of the evolution of planetary atmospheres envisage the formation of the atmospheres of the inner planets by slow emission of gases from the crust. It is conjectured that the gases emerging from the Earth’s crust, including water vapour, are those found in its atmosphere today, whereas those of both Venus and Mars have since lost their water vapour content. In the beginning, the atmospheres of the three inner planets were cold, the atmospheric pressure low, and $\tau^* \ll 1$. The early surface temperatures of each planet increased with the release of water vapour to the atmosphere by virtue of the greenhouse effect. The general idea is that the growth of atmospheric pressure and temperature on Earth was arrested either by freezing or by condensation of water vapour forming clouds that ultimately produced rainfall and the oceans of the world. This evolutionary process is referred to as a truncated greenhouse effect (Fig. 5). It is this abrupt termination

to the evolution of the Earth's greenhouse that is thought to have buffered the Earth's climate from large variations.

Because Venus is closer to the sun, its primitive state was warmer than that of Earth. Consequently, much more water vapour would have been needed for condensation to occur. One school of thought proposes that water vapour concentrations increased systematically in the early atmosphere of Venus without ever reaching condensation. This increase led to an increase in τ^* which further enhanced the greenhouse effect on Venus. This enhancement in turn led to higher surface temperatures allowing the atmosphere to hold even more vapour, creating a positive feedback cycle with the atmosphere never reaching saturation. This state is referred to as the runaway greenhouse effect, as illustrated in Fig. 5, and it is speculated that this runaway greenhouse effect on Venus prevented oceans from ever forming on that planet. As part of this conjecture, it is generally supposed that water vapour in the atmosphere of Venus photodissociated, with H^+ escaping to space and with O_2 being fixed in rocks. It is postulated that during the course of this proposed hydrodynamic loss, the surface temperatures of Venus became high enough to create a kind of chemical equilibrium between atmospheric gases and the surface. In the course of these chemical reactions, enough condensed material accumulated in the atmosphere to form the extensive clouds that cover Venus today. The current explanations for the large values of τ^* that sustain the present greenhouse effect on Venus reside in the belief that the clouds of Venus perform a similar function to water vapour in the primitive atmosphere. The presence of large concentrations of CO_2 in the atmosphere of Venus also contributes significantly to this effect, but absorption by CO_2 is spectrally too narrow to provide the values of τ^* that are necessary to explain the observed temperatures on Venus.

The evolution of the atmosphere of Venus is a subject of some debate. Conjectures other than the runaway greenhouse–hydrodynamic loss hypothesis have been put forward to explain the present climate of Venus. A contrary view is that the atmosphere of Venus never contained water vapour at the levels required for the runaway hypothesis and that most of the planet's water remains fixed in its interior (Kaula 1990).

Whether this runaway greenhouse model proposed for Venus actually occurred is not the issue here. The runaway hypothesis serves to illustrate a feedback between water vapour, the greenhouse effect and the surface temperature of the planet; a feedback that is also thought to occur on Earth although on a much more limited scale (Manabe and Wetherald 1967). In fact, it is the water vapour feedback in present day climate models that contributes the major portion of the global warming predicted for increasing concentrations of atmospheric CO_2 . Fig. 6a provides a schematic depiction of how this water vapour feedback is thought to take place under the influence of increasing concentrations of carbon dioxide. As the sea surface temperature warms due to the rising levels of CO_2 , increased evaporation of water from the oceans leads to an enhanced water vapour content of the atmosphere (Fig. 6a) which further warms the oceans. The total warming calculated by a typical climate model is also given in Fig 6a, as is the amount of warming calculated for a doubling of CO_2 without any water vapour feedback. While these results apply to a specific climate model (Ramanathan 1981) they are typical of other models which predict that more than

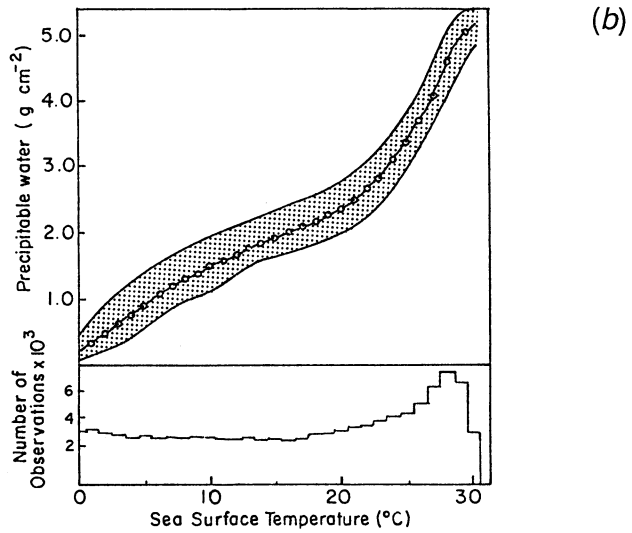
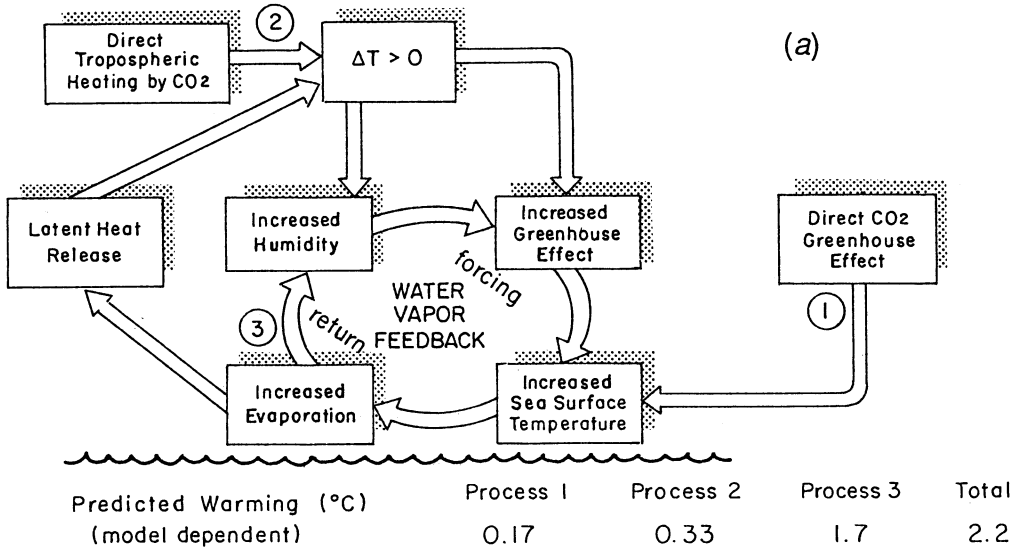


Fig. 6. (a) An illustration of the water vapour feedback as it is thought to occur on Earth when triggered by a small warming induced by increasing atmospheric CO₂. The water vapour feedback is thought to account for more than half the final warming simulated by present-day climate models [adapted from Ramanathan (see Manabe and Wetherald 1967)]. (b) A necessary condition for the existence of water vapour feedback on Earth. Water vapour exists in equilibrium with the oceans in a way that is related to the sea surface temperature, essentially in line with the Clausius-Clapeyron relationship. The curve shown is established from thousands of observations of water vapour over the world's oceans (Schneider 1990).

half the projected global warming due to increasing carbon dioxide occurs through the effects of the water vapour feedback.* An important component of the feedback is contained in the assumption that a warmer atmosphere contains more water vapour. Observations, like those shown in Fig. 6b, suggest that a kind of thermodynamic equilibrium exists between the sea surface temperature and water vapour content similar to that described by the Clausius–Clapeyron relation.

Unlike the case for Venus, however, the water vapour feedback loop on Earth is interfered with by condensation of vapour into clouds which, in turn, impart a substantial influence of their own on the greenhouse effect. The actual way this interference by clouds takes place and the specific connection between water vapour, cloudiness and the greenhouse effect on Earth are still not understood.

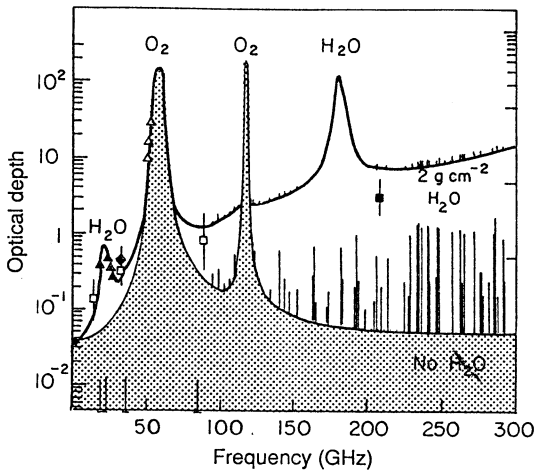


Fig. 7. Absorption spectrum of the atmosphere at microwave frequencies highlighting the location of the four SSMI channels at 19.35, 22.235, 37 and 85.5 GHz. Located at 22.235 GHz is a weak absorption line and the absorption–emission from this line is utilised in retrieving precipitable water. Another feature also used in the remote sensing of the Earth’s atmosphere is the band of absorption lines due to rotational transitions of the O_2 molecule at 60 GHz.

4. Observations of the Greenhouse Effect of Earth

Knowledge about how water vapour is distributed in the atmosphere, how it is transported by atmospheric motions and, perhaps most importantly of all, how it is transformed into clouds is fundamental both to understanding the Earth’s greenhouse effect and how it is likely to evolve in the future. Unfortunately, water vapour is notoriously difficult to measure and routine observations from balloons are limited in both their spatial and temporal coverage, generally being accurate to no better than about 10% and biased to the large land masses of the Northern Hemisphere (Trenberth *et al.* 1987). Recent advances in both satellite observations and in the interpretation of these observations now provide us with a much more complete global coverage of water vapour levels with an accuracy no worse than that of balloon observations. Perhaps the most direct and unambiguous estimate of

* Other views have been expressed that the positive feedback does not operate to the extent predicted in current climate models. For further discussion see Schneider (1990).

the precipitable water content w is provided by satellite measurements of the microwave radiation emitted by the Earth to space. In July 1987 the Special Sensor Microwave Imager (SSMI) was launched as part of the US Defense Military Satellite Program (DMSP). This microwave instrument on the satellite provides almost global coverage of the microwave emission at four frequencies (Fig. 7). Measurements near the water vapour absorption line centred at 22.235 GHz are used to derive the precipitable water (Stephens 1991; Stephens and Greenwald

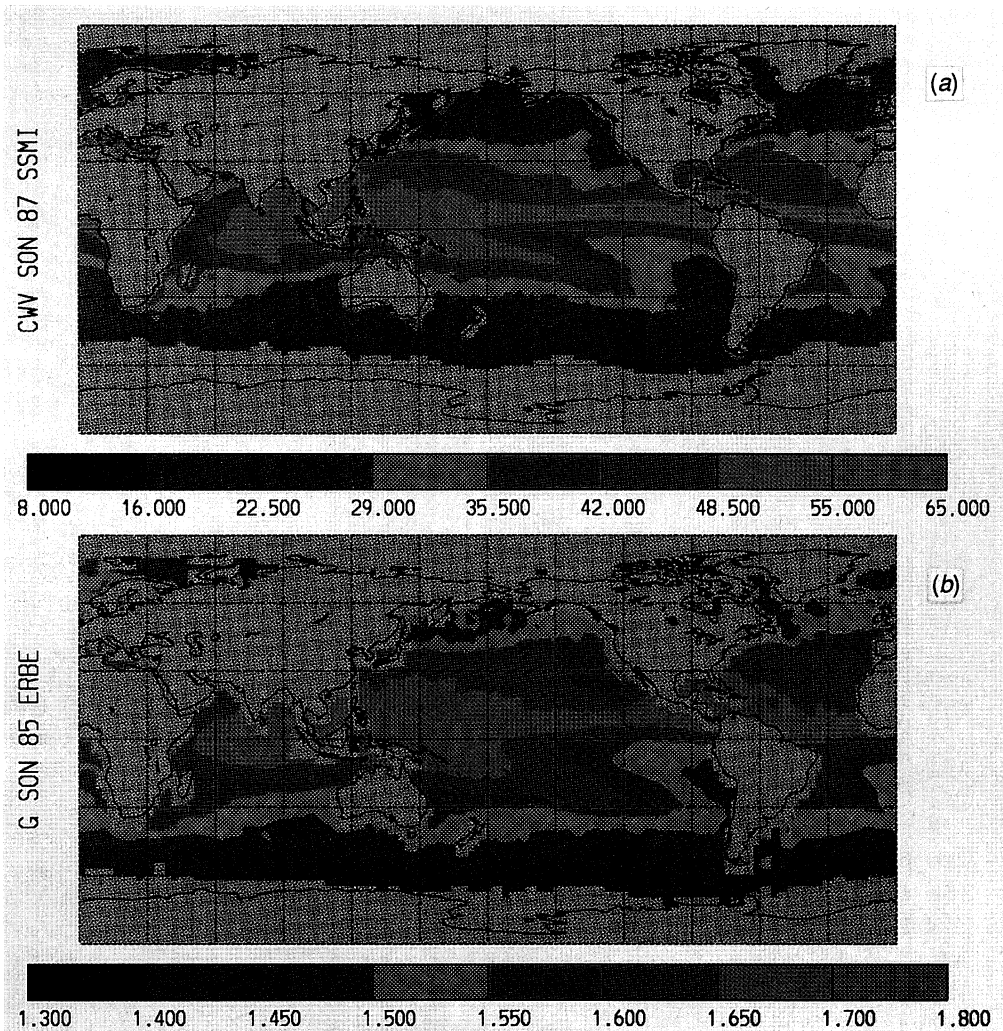


Fig. 8. (a) Distribution of precipitable water (colour scale corresponds to units of kg m^{-2}) derived from SSMI observations over the world's oceans for the 1987 SON season. The region of highest moisture is located over the equatorial western Pacific where the warmest sea surface temperatures are found on Earth. (b) Distribution of the greenhouse effect G as defined by (14) over the world's oceans for clear skies for the 1979 SON season. The largest values of G are found in the equatorial regions which have the largest values of w .

1990; Chang and Wilhelm 1979). The retrieval of w from these measurements is relatively straightforward over the oceans where the emission of microwave radiation from the ocean surface is readily estimated. Unfortunately, this is not the case over land, where microwave emission is much more variable, depending on soil type, soil moisture, vegetation and other factors. At present, it has not been possible to obtain a truly global distribution of water vapour from microwave satellite observations. The infrared observations from operational satellites (Prabhakara *et al.* 1980; Hayden *et al.* 1981) provide better spatial coverage of water vapour information for global climate studies. However, the accuracy of the infrared water vapour data, retrieval biases introduced by avoidance of cloudy regions and the sensitivity of the retrieval methods to initial conditions need to be established before these data can be used for climate studies of water vapour.

An example of a seasonally averaged distribution of precipitable water vapour is presented in Fig. 8*a*. This seasonal distribution is defined from the September, October and November monthly averages of the SSMI observations. No information about water vapour is provided over land. One of the predominant features of this distribution is the large region over the equatorial Western Pacific that contains more than 5 g cm^{-2} of water vapour. Also evident is the drier air just west of the coasts of North and South America and Africa which overlies the colder waters that occur due to the upwelling of deep ocean waters in these regions. The distribution of the clear-sky greenhouse effect as defined by (14) is presented in Fig. 8*b* for comparison. The values of \mathcal{G} presented in this diagram are calculated from the observations of the sea surface temperature and the measurements of clear-sky longwave emission to space which are obtained from measurements of the Earth's radiation budget like those described by Ramanathan *et al.* 1989).

There is a remarkable correspondence between the distribution patterns of \mathcal{G} and the distribution patterns of w . Our simple model of the Earth's greenhouse effect predicts a relationship between the clear-sky \mathcal{G} and the precipitable water w of the form

$$\mathcal{G} = a + cw, \quad (15)$$

where we combine (6) and (14) to produce (15). This is a particularly useful relationship as we are able to test our simple model with the observations used to produce Fig. 8. Examples of the correlation of \mathcal{G} , derived from Earth radiation budget and sea surface temperature observations, and using coincident microwave observations of w , are given in Fig. 9 for the two seasons indicated. These results indicate that the observations of the greenhouse effect on Earth obey the type of relationship predicted by (15) for clear skies.

Stephens and Greenwald (1991) provided a theoretical account of (15) and the factors that affect the numerical values of a and c . They demonstrated that the slope factor c is largely governed by the variation of temperature with height in the atmosphere (the lapse rate) and that the intercept a is determined by a variety of factors including the assumed profile of water vapour as well as the concentrations of other greenhouse gases. Whether present-day global climate models predict values of a and c similar to those observed remains a matter for future research.

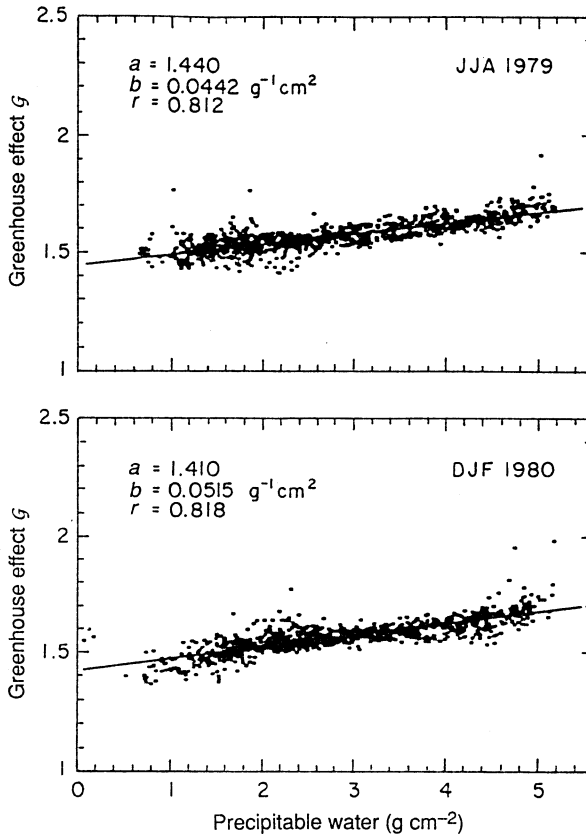


Fig. 9. Correlations between the observed greenhouse effect and the vertically integrated atmospheric water vapour content for the 1979/80 DJF and 1979 JJA seasons. The water vapour data were obtained from a different set of microwave observations to those shown in Fig. 8a. The numerical values of the coefficients given in equation (15) as well as the correlation coefficient are given.

5. Discussion

What can we learn about the water vapour feedback mechanism from such observations? Unfortunately, it is not possible to observe the water vapour feedback directly, as the observed correlations with the greenhouse effect are a consequence not only of the water vapour feedback but also of other processes and feedbacks. The relationship between \mathcal{G} and sea surface temperature T_s is composed of two important factors; one deals with how the greenhouse effect is influenced by water vapour and the second deals with how water vapour, in turn, is affected by a change in surface temperature resulting from a change in the greenhouse effect. Namely,

$$\frac{d\mathcal{G}}{dT_s} = \frac{d\mathcal{G}}{dw} \frac{dw}{dT_s}, \quad (16)$$

where the first factor on the right-hand side of (16) represents the observed

coupling between \mathcal{G} and w shown in Fig. 9, and the second factor represents the relationship shown in Fig. 6b.

If we assume that the relationship between w and T_s has the form (Stephens 1990)

$$w = d \exp[r(T_s - 288)], \quad (17)$$

then substituting (15) and (17) in (16) leads to

$$g = \frac{d\mathcal{G}}{dT_s} = cdr \exp[r(T_s - 288)], \quad (18)$$

which is the sensitivity of the greenhouse effect to changes in sea surface temperature. As an illustration, if we assume that the global mean SST is 292 K, then $g = 0.012 \text{ K}^{-1}$, based on a least-squares fit to the observations.

The sensitivity relationship (18) establishes an important property of the Earth's greenhouse: that its sensitivity to changing sea surface temperature is not uniform over the globe but is significantly greater over the warmest oceans. If we believe the present sensitivities derived in this way, then monitoring w especially over the warmest ocean waters may also provide an early way of detecting climate change.

The sensitivity parameter defined above and estimated from data should not be misconstrued as a measure of feedback between \mathcal{G} and the sea surface temperature. A number of factors other than sea surface temperature may also influence the observed distributions of \mathcal{G} and thus the parameter g . Among these factors are the vertical profiles of water vapour* and temperature, and variations in spectroscopic parameters with height. The parameters used to estimate g in this study correspond to a set of conditions that do not remain fixed but vary in a way associated with changing sea surface temperature. A fundamental issue, and a topic of a further study, concerns the robustness of the relationship shown here and whether the same sensitivities derive from climate states that are different from the observed present-day state.

Acknowledgments

Portions of the research described in this paper are supported by NOAA Grant #NA90AA-D-AC822.

References

- Arrhenius, S. (1896). *Philos. Mag.* **41**, 237.
 Bohren, C. F. (1987). 'Clouds in a Glass of Beer', p. 83 (Wiley: New York).
 Callender, G. S. (1938). *Quart. J. Roy. Meteor. Soc.* **64**, 223.

* Lindzen (1990) argues that the water vapour feedback is sensitive to how water vapour is distributed in the vertical. The greenhouse effect is more sensitive to changes in a relatively small amount of vapour high in the troposphere than to larger changes of water vapour lower in the atmosphere. The extent to which the vertical distribution of water vapour varies globally and the factors that govern this variability are not well known nor well studied at this point.

- Cess, R. D. *et al.* (1990). *J. Geophys. Res.* **95** (D10), 16601.
- Chang, A. T. C., and Wilheit, T. T. (1979). *Radio Sci.* **14**, 793.
- Dines, W. H. (1917). *Quart. J. Roy. Meteor. Soc.* **43**, 151.
- Foukal, P. V. (1990). *Sci. Amer.* (Feb.), 34.
- Fourier, J. B. (1787). *Acad. Sci. Instr. Fr.* **7**, 569.
- Goody, R. M., and Walker, J. C. G. (1972). 'Atmospheres', (Prentice Hall: New York).
- Goody, R. M., and Yung, Y. L. (1989). 'Atmospheric Radiation—Theoretical Basis' (Oxford Univ. Press).
- Hanel, R. A. (1983). In 'Spectrometric Techniques', Vol. 3 (Ed. G. A. Vanasse) (Academic: New York).
- Hayden, C. M., Smith, W. L., and Wolf, H. M. (1981). *J. Appl. Meteor.* **20**, 155.
- Kaula, W. M. (1990). *Science* **247**, 1191.
- Lindzen, R. S. (1990). *Bull. Am. Meteor. Soc.* **71**, 288.
- Manabe, S., and Wetherald, R. T. (1967). *J. Atmos. Sci.* **24**, 241.
- Mihalas, D. (1978). 'Stellar Atmospheres' (Freeman: San Francisco).
- Moroz, V. I., *et al.* (1986). *Appl. Opt.* **25**, 1710.
- Prabhakara, C., Chang, H. D., and Chang, A. T. C. (1980). *J. Appl. Meteor.* **21**, 59.
- Ramanathan, V. (1981). *J. Atmos. Sci.* **38**, 918.
- Ramanathan, V. (1988). *Science* **240**, 293.
- Ramanathan, V., Barkstrom, B. R., and Harrison, E. F. (1989). *Physics Today* (May), 22.
- Rasool, S. I., and DeBergh, C. (1990). *Nature* **226**, 1191.
- Rothman, L. S. (1981). *Appl. Opt.* **20**, 802.
- Schneider, S. H. (1990). *Bull. Am. Meteor. Soc.* **71**, 1292.
- Stephens, G. L. (1990). *J. Climate* **3**, 634.
- Stephens, G. L., Campbell, G. C., and Vonder Haar, T. H. (1981). *J. Geophys. Res.* **86**, 9739.
- Stephens, G. L., and Greenwald, T. J. (1991). *J. Geophys. Res.* **96**, 15311.
- Trenberth, K. E., Christy, J. R., and Olsen, J. G. (1987). *J. Geophys. Res.* **92**, 14815.
- Vonder Haar, T. H., and Suomi, V. (1971). *J. Atmos. Sci.* **28**, 305.